ELSEVIER

Journal of Nuclear Materials 258–263 (1998) 173–182

journal of nuclear materials

Impacts of charge-exchange neutrals on degradation of plasma-facing materials

N. Yoshida [a,*], Y. Hirooka [b]

[a] *Research Institute for Applied Mechanics, Kyushu University, Kasuga, Fukuoka 816-8580, Japan*

[b] *Department of Applied Mechanics and Engineering Sciences, University of California, San Diego, 9500 Gilman Dr., La Jolla, CA 92093-0417, USA*

Abstract

This paper reviews the recent data from the PISCES linear plasma facility and the TRIAM-1M tokamak, demonstrating the impacts of energetic charge-exchange particles on surface erosion and bulk damage. High energy neutrals can result in significant surface erosion via sputtering even for tungsten. For the erosion of tungsten it has been emphasized in the PISCES data that oxygen-containing plasma impurities dominate the overall erosion behavior at energies below the sputtering thresholds for hydrogenic species. Radiation damage has been observed in plasma-facing materials in TRIAM-1M due to charge-exchange hydrogen neutrals. The accumulation of dislocation loops has been observed in metals subjected to the bombardment of charge-exchange hydrogen neutrals with energy up to keV. The flux was on the order of 10^{18} H atoms/m^2/s, which is comparable with the ITER first wall condition. Severe embrittlement was observed in tungsten after long-term exposure in TRIAM-1M. Due to their strong interaction with lattice defects, helium atoms cause more profound effects on material properties than hydrogen. Defect accumulation by keV helium ions induces significant hardening and embrittlement even at high temperatures. As such, bombardment of energetic neutrals of hydrogen and helium can result in unrecoverable damage in plasma-facing materials and degrade even material bulk properties. © 1998 Published by Elsevier Science B.V. All rights reserved.

1. Introduction

In the presently operating fusion devices as well as future power reactors, plasma-facing materials will be subjected to high-flux particle bombardment, including ions and neutrals of fuel hydrogen isotope and helium ash, though their flux and energy characteristics depend on the plasma position. In the case of ITER, for example, the flux and average energy of hydrogen ions bombarding divertor plates are estimated to be $<10^{24}$ ions/m^2/s and <100 eV [1]. Therefore the main concern for the divertor materials is sputtering erosion by these high flux ions. The utilization of high-Z materials such as tungsten, which has a high sputtering threshold, has been considered as a possible way of overcoming the sputtering erosion. The situation for the first wall is considerably different from the divertor plate. The flux and energy of hydrogenic species bombarding the first wall of ITER are estimated as $<10^{20}$ particles/m^2/s and 100–500 eV, respectively [1]. These particles are charge-exchange hydrogen neutrals produced in the edge plasma. More details estimated recently are: the flux of neutrals is 10^{18}–10^{19} atoms/m^2/s for around 100 eV and 5×10^{18}–5×10^{19} atoms/m^2/s for around 5 eV [2]. In addition to these rather low energy charge-exchange neutrals, high-energy neutrals escaping from the high temperature core plasma will also impinge on the first wall. Their flux and energy are predicted to be the order of 10^{18} atoms/m^2/s and 10 keV, respectively. Though the flux of the neutrals is much less than that of the ions, they can result in significant sputtering erosion as well as knock-on damage in the materials.

Effects of particle bombardment on plasma-facing materials have been examined extensively, focusing on surface erosion and impurity emission [3,4]. These studies were motivated to improve plasma cleanliness.

* Corresponding author. Tel.: +81 92 583 7716; fax: +81 92 583 7690; e-mail: yoshida@riam.kyushu-u.ac.jp.

0022-3115/98/$19.00 © 1998 Published by Elsevier Science B.V. All rights reserved.
PII: S0022-3115(98)00268-2

Mayer et al. [5] observed significant sputtering erosion at the vessel wall of JET by charge-exchange neutrals. They emphasized the important roles of charge-exchange neutrals in the first wall erosion and of resultant impurity ejection into the plasma. On the other hand, it has been reported that tokamak plasma exposure can produce remarkable knock-on damage in the sub-surface region of plasma-facing materials [6–9].

In this paper, therefore, recent studies on sputtering erosion and radiation damage in steady-state plasma devices will be reviewed, emphasizing the role of energetic charge-exchange neutrals of hydrogen and helium in the property degradation processes of plasma-facing materials.

2. Surface erosion of plasma-facing components by charge-exchange neutrals

The difficulty of handling charge-exchange neutrals is that magnetic confinement cannot control their interactions with plasma-facing components. It follows directly from this that the sputtering of plasma-facing materials by these charge-exchange neutrals is unavoidable. The energies of these neutrals are determined essentially by the plasma temperature in the region where charge-exchange reactions occur. This means that the particle bombarding energy to the materials surface ranges up to keV even though the edge temperature may be reduced to a few eV by applying the radiative mode of operation. Therefore, it is desirable that the materials erosion yield is not a steep function of particle bombarding energy. In this section, the existing erosion database on tungsten and beryllium will be reviewed, taking into account the effects of plasma impurities.

Shown in Fig. 1 is the erosion behavior of tungsten under oxygen-contaminated deuterium plasma bombardment at 1500°C [10]. The tungsten materials used in these experiments were in the form of 1 mm thick high-pressure-sintered bulk-material and 1 mm thick coatings on molybdenum prepared by the CVD and plasma-spray methods. Important experimental conditions are listed in Table 1. Taking into account the effect of plasma impurities, the total materials erosion rate is generally expressed as follows [11]:

$$\Gamma_{\text{total}} = \Sigma\Gamma_{\text{D,T}}\left\{ Y_{\text{D,T}} + \Sigma\left(\frac{\Gamma_i}{\Gamma_{\text{D,T}}}\right) Y_{\text{i}} \right\}, \tag{1}$$

where Γ_{total} is the total rate of materials erosion, $\Sigma\,\Gamma_{\text{D,T}}$ is the flux of DT-particles, $\Sigma\Gamma_i$ is the flux of impurity particles, $Y_{\text{D,T}}$ is the sputtering yield due to DT particles; and Y_{i} is the sputtering yield due to impurity particles. From Eq. (1) the "effective" erosion yield by the D,T particle bombardment is defined as follows:

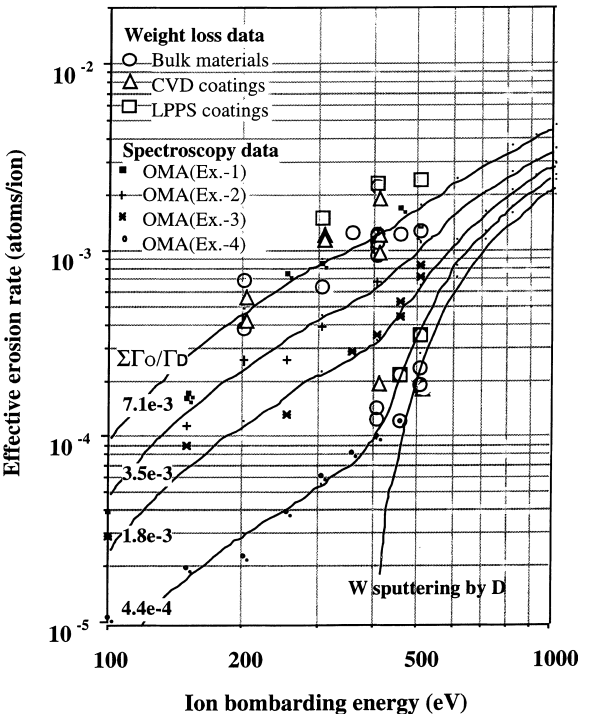

Fig. 1. Effective erosion rate data for tungsten bombarded with oxygen-contaminated deuterium plasmas in the PISCES-B facility [1].

$$Y_{\text{eff}} \equiv Y_{\text{D,T}} + \Sigma\left(\frac{\Gamma_i}{\Gamma_{\text{D,T}}}\right) Y_{\text{i}}. \tag{2}$$

Plotted in Fig. 1 are the effective erosion yield data for tungsten:

$$Y_{\text{W-eff}} \equiv Y_{\text{D}} + \left(\frac{\Sigma\Gamma_0}{\Gamma_{\text{D}}}\right) Y_0 \tag{3}$$

in the oxygen-to-deuterium plasma flux ratio range from 4.4×10^{-4} to 7.1×10^{-3}.

Important findings are as follows. Despite their low concentration, oxygen-containing plasma impurities dominate the total erosion of tungsten, particularly at relatively low energies below around the sputtering threshold energy for deuterium. Also, notice that the effective erosion yield data obtained for different forms of tungsten are essentially the same, meaning that momentum transfer processes associated with sputtering do not strongly depend on materials bulk properties. To corroborate these laboratory experiment data, as shown in Fig. 2, the recent measurements in the ASDEX-Upgrade tokamak have indicated that multiple-charged carbon impurities dominate the erosion of 0.5 mm thick plasma-sprayed tungsten coatings used for the divertor plate [12].

Table 1
Experimental conditions in the PISCES-B Mod facility

Parameters	Achievable	Applied here
Plasma species	H,D,He,Ar,N	D + (C, O)-impurities
Pulse duration (s)	Continuous	Up to 3600
Plasma density (cm^{-3})	Up to 3×10^{13} (D)	5×10^{11}–4×10^{12}
Electron temperature (eV)	5–30	5–15
Ion bombarding flux (ions/cm^2/s)	up to 3×10^{19}	5×10^{17}–3×10^{18}
Ion bombarding energy (eV)	30–500 (dc bias)	100–500
Surface temperature (°C)	R.T. - 1600	R.T. - 1500

Samples. Tungsten: (1) 1 mm thick sheet prepared by high pressure sintering (Johnson Matthey); (2) 1 mm thick coatings prepared by chemical vapor deposition (ULTRAMET); (3) 1 mm thick coatings prepared by low pressure plasma spray (Electro Plasma). Beryllium: (1) 1 mm thick sheet prepared by hot pressed powder metallurgy (S65-B:BrushWellman).

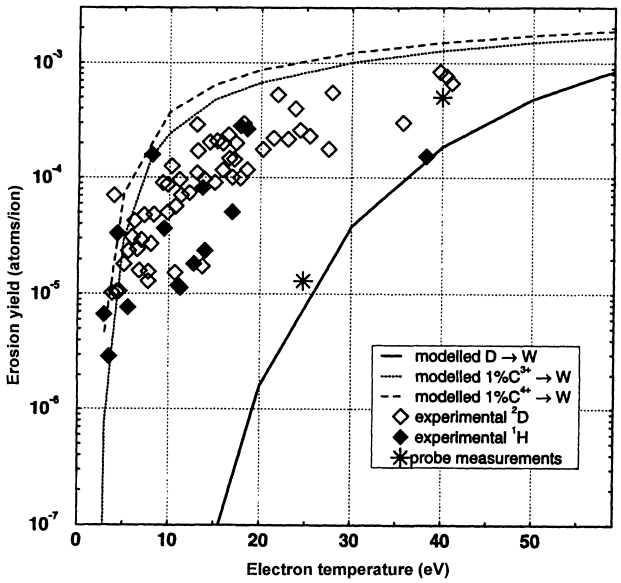

Fig. 2. Effective erosion yield data for plasma-sprayed tungsten coatings used for the divertor plate in the ASDEX-Upgrade tokamak [3].

Shown in Fig. 3 are the effective erosion yield data taken for beryllium under carbon-contaminated deuterium plasma bombardment [13]. Experimental conditions are listed in Table 1. As for interaction behavior with plasma impurities, beryllium is rather different from tungsten. Although details can be found elsewhere [11,14], the difference between these two materials is briefly mentioned here for completeness. From the materials mixing model, the critical carbon impurity content required for film deposition on beryllium has been calculated to be 0.01 in terms of $\Sigma\Gamma_C/\Gamma_D$ [14], which is likely for a large fusion device whether or not carbon is used for plasma-facing components. The corresponding value for tungsten is nearly an order of magnitude higher, indicating the substrate mass effect on carbon deposition efficiency. It follows directly from this that beryllium tends to be contaminated with the deposition of carbon-containing impurities, particularly at elevated temperatures where materials mixing due to thermal diffusion becomes important [11,14]. Once carbon deposition occurs, substrate materials erosion is significantly suppressed due to the mixing effect. In fact, the reduced erosion of beryllium plasma-facing components has recently been observed in the JET tokamak [15], corroborating these laboratory data and modeling analysis.

Importantly, however, until their concentration reaches the critical level for film deposition, carbon impurities will enhance erosion, as demonstrated for tungsten in this section. The erosion yield data shown in Fig. 3 include those taken with carbon deposition at elevated temperatures as well as those without it at room temperature. Importantly, even without carbon redeposition effective erosion data indicate the effect of

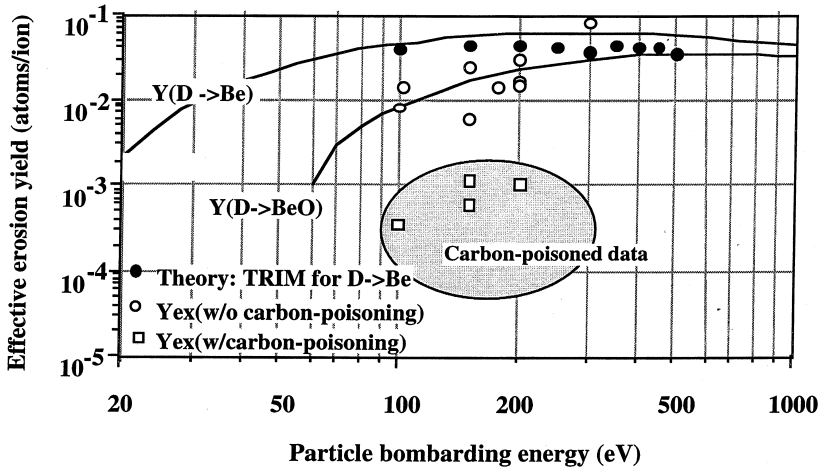

Fig. 3. Effective erosion yield data for beryllium bombarded with carbon-contaminated deuterium plasmas in the PISCES-B facility [3].

beryllium oxide formation resulting in somewhat reduced sputtering.

Turning to the effect of high-energy charge-exchange neutrals on materials erosion, the energy dependence of erosion yield is the key information. As can be seen in Fig. 1, the effective erosion yield for tungsten is a rather steep function of bombarding energy. As bombarding energy increases, deuterium begins to take place for oxygen impurities, governing the overall erosion behavior. It is critically important to note here that unless they are singly charged ions, plasma-impurities are not likely to contribute to increasing the high-energy charge-exchange neutral flux. Therefore, the fact that tungsten erosion becomes substantial and dominated by deuterium at high energies deserves a caution from reactor designers in materials selection and positioning of plasma-facing components. In the case of beryllium, however, the erosion yield does not exhibit a steep increase with increasing bombarding energy whether or not carbon deposition occurs. This means that beryllium erosion will not be strongly influenced by high-energy charge exchange neutrals.

3. Radiation damage in TRIAM-1M tokamak under long discharges

The TRIAM-1M tokamak has Nb_3Sn superconducting poloidal magnets, producing a toroidal field of 8 T [16]. This device is suitable for plasma-wall interactions research due to steady state discharges with a duration of more than 2 h heated by lower-hybrid current drive (LHCD) [17]. A collector probe, on which several kind of pre-thinned metal specimens were mounted, was inserted in the scrape-off layer (SOL) of TRIAM-1M through a horizontal port using a high-vacuum sample transfer system. These specimens were exposed to long pulse discharges with following parameters; $I_p = 23$–25 kA, $\overline{n_e} = 2 \times 10^{18}/m^3$, $T_i = 0.6$ keV. After exposure the specimens were taken out from the probe and were examined by transmission electron microscopy (TEM).

Radiation-induced defects have been observed in many metals such as aluminum, copper, stainless steel, molybdenum and tungsten [8,9]. Shown in Fig. 4 are typical TEM images of tungsten exposed to a steady state plasma for 72.1 min [18]. Small but dense defect clusters with white dot images or white ring images are observed (average diameter $\approx$ 10 nm, areal density $\approx$ $2 \times 10^{15}/m^2$). Stereoscopic analysis has shown that they appear to be locally formed in the sub-surface layer of about 60 nm thick. The image and thermal mobility of the point defects indicate that they should be the clusters of interstitials, which have been introduced by the knock-ons with energetic particles. The depth distribution of the defects indicates that the hydrogen particles should be responsible for the damage formation [9].

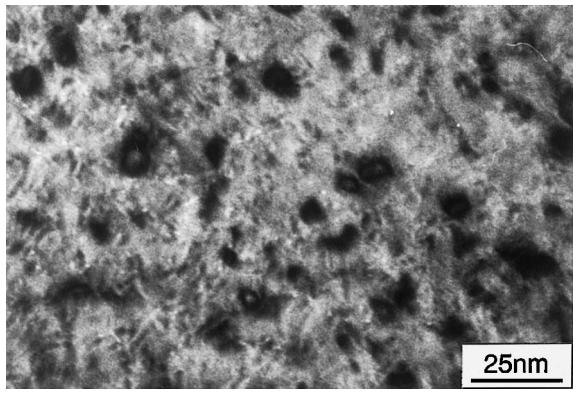

Fig. 4. Dislocation loops formed in tungsten by 72.1 min-discharge in TRIAM-1M [18].

The formation and accumulation of lattice damages depend strongly on the incident particle energy. In the case of tungsten, as will be described in detail in the following sections, there is a clear energy dependence; interstitial loops are formed above 3 keV but not below 2 keV (see Fig. 8). This indicates that hydrogen particles probably have energies above 2–3 keV and can then result in remarkable knock-on damage even in high-Z materials as such tungsten.

Fig. 5 shows position dependence of radiation damage produced in aluminum specimens exposed to a TRIAM-1M plasma for about 22 min at various positions [9]. The position is denoted as *P*-5.0 mm in the figure, where *P* and *I* present plasma-facing side and ion drift side, respectively. The number indicates the distance from the limiter surface. Because of the wall position was at 10 mm, the specimens between 0 and 10 mm were located in the SOL. Radiation induced interstitial type dislocation loops were formed not only on the plasma-facing side in the SOL (*P*-5.0 mm) but also inside a port (*I*-12.5 mm and *I*-15.5 mm), where ionized particles hardly reach due to magnetic confinement, excepting some low energy ions in the boundary plasma as sheath current. The specimen placed on the ion drift side in the SOL (*I*-9.5 mm) was covered by a thick redeposited impurity layer. This result implies that the energetic particles causing the damage are neutrals but not ions.

In order to estimate the flux of the energetic hydrogen neutrals responsible for the damage formation, the data of the TRIAM-1M experiments were compared with those of the simulation experiments with hydrogen ion beams, which will be explained in more detail in the following section [19]. In Fig. 6, the defect density and average size in molybdenum formed due to plasma exposure and from those of the simulated irradiation at several different energies are plotted together. Both density and average size of the TRIAM-1M experiment correspond well with those of 0.5 and 2 keV at the fluence of about $2–4 \times 10^{21}$ H^+/m^2. Because of wide energy spectrum for tokamak plasma it is impossible to estimate the energy and flux rigorously from such comparison but we may say roughly that hydrogen neutrals at around 0.5–3 keV bombard the wall with a flux of about $1.5–3 \times 10^{18}$ $H/m^2/s$. This corresponds about $3–6 \times 10^{-4}$ dpa/s at the peak for molybdenum and about 0.4–0.8 dpa for 22 min-discharge. As discussed in the following sections, accumulation of dislocation loops reaches the maximum by the irradiation of about 10^{22} H^+/m^2 and induces remarkable change of mechanical properties of sub-surface region. This means that surface properties may change remarkably within a few tens of hours discharges in TRIAM-1M.

These experimental data indicate that energetic charge-exchange hydrogen neutrals ejected from the core plasma can result in knock-on damage in the subsurface region of the plasma facing wall and a heavy damage is accumulated in a short experimental period. This effect is unavoidable in any tokamaks because the charge-exchange neutrals cannot be confined by the magnetic field.

Thin edges of tungsten specimens placed on the first wall for 3 months was broken along grain boundaries. Such phenomenon is often observed in tungsten irradiated with energetic hydrogen ions at rather low temperatures. We should note that influences of the energetic hydrogen influx are not restricted in the shallow sub-surface range but may change even the properties of bulk materials.

4. Radiation damage by keV-range energy hydrogen particles

To simulate the evaluation of radiation damage during plasma exposure, hydrogen ion irradiation has

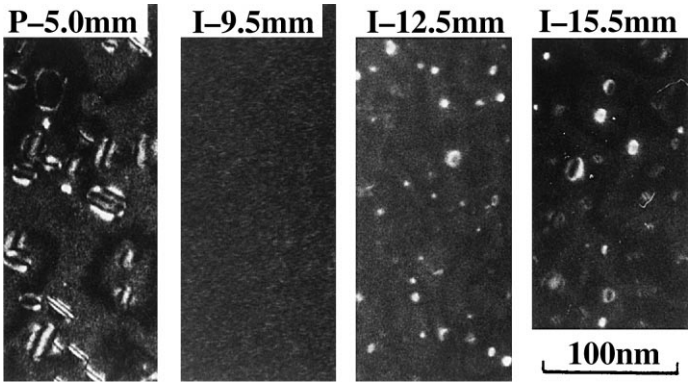

Fig. 5. Interstitial type dislocation loops formed in aluminum placed at the plasma facing side in SOL (*P*-5.0 mm) and at the ion drift side (*I*-9.5 mm, *I*-12.5 mm, *I*-15.5 mm) by 22 min-discharges of TRIAM-1M.

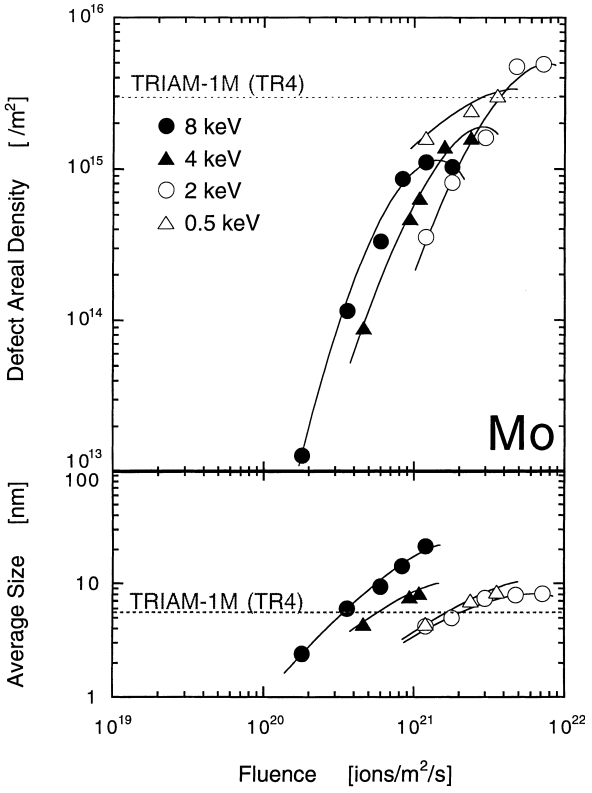

Fig. 6. Density and average size of the defects in molybdenum formed by 22 min-discharge of TRIAM-1M (dashed lines) and those by hydrogen ion irradiation at several energy.

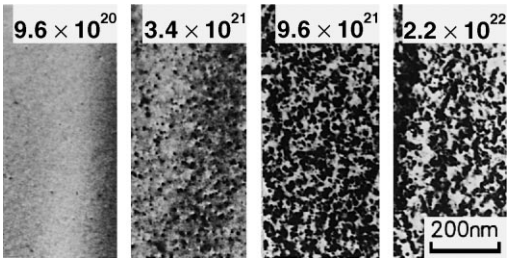

Fig. 7. Microstructural evolution of molybdenum at room temperature during irradiation with 2 keV H^+ ions (2×10^{18} ions/m^2/s). The number in the figure denotes hydrogen fluence (ions/m^2).

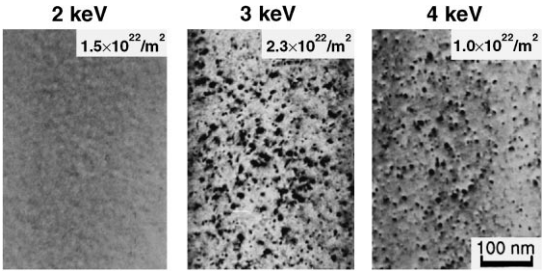

Fig. 8. Ion energy dependence of microstructure in tungsten formed by H^+ ion irradiation at room temperature.

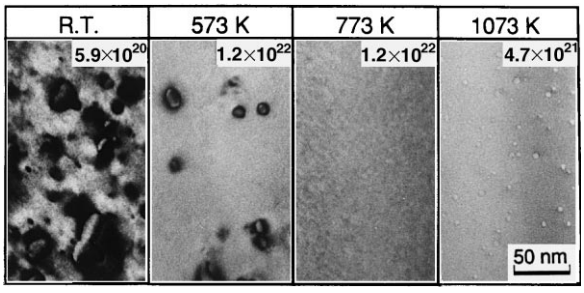

Fig. 9. Temperature dependence of microstructure of tungsten during irradiation with 8 keV hydrogen ions.

been carried out simultaneously with transmission electron microscopy [19,20]. Fig. 7 shows typical evolution in molybdenum at room temperature under irradiation with H^+ ions at 2 keV. Defects with black dot contrast are formed at a low fluence and their density saturate at about 1×10^{22} ions/m^2, forming a tangled dislocation structure. In the case of tungsten, damage evolution shows very clear ion energy dependence as shown in Fig. 8 [20]. Dislocation loops are formed above 3 keV but not below 2 keV, because the displacement threshold energy is 44 eV [21], which requires hydrogen ions to be higher than 2.05 keV.

Microstructural evolution depends on irradiation temperature as demonstrated in Fig. 9. In the case of tungsten irradiated by 8 keV-H^+, dislocation loops, which are major defects at lower temperatures, are scarcely formed above 773 K, while fine cavities of about a few nm are slowly formed above 873 K. If the cavities remain at these levels of size and density, the influence of hydrogen particle loading on material properties seems negligible, but one should pay attention to their evolution at higher fusion relevant fluences.

Beryllium shows rather different behavior under hydrogen ion irradiation. The radiation damage produced in beryllium by 8 keV-D_2^+ irradiation is shown in Fig. 10 [22]. Bubbles and/or cavities are formed at all temperatures up to 873 K. For example, local swelling by the bubbles exceeds 30% at 573 K. A similar bubble formation occurs by 0.2 keV-D_2^+ irradiation, but at a slower rate. As shown in Fig. 11, a large amount of injected deuterium atoms are trapped in the bubbles up to 673 K. Thermal desorption data indicate that deuterium is detrapped between 800 and 1000 K during the temperature ramp. This means that hydrogen particles, even if their energy is rather low, form bubbles at the sub-surface region of a beryllium wall, and the defects act as strong trapping sites for hydrogen isotopes even in the

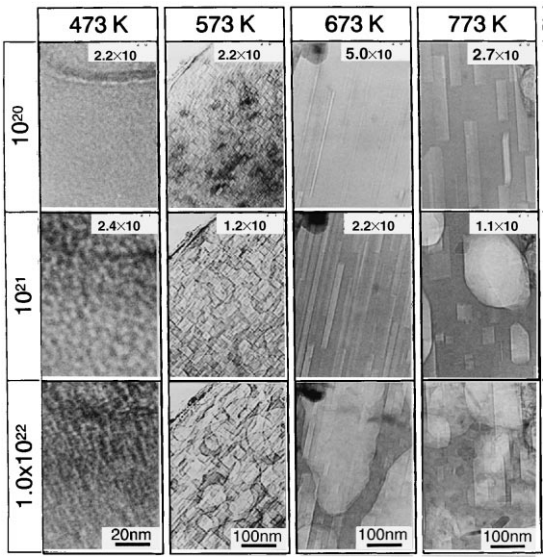

Fig. 10. Microstructural evolution in beryllium by 8 keV-D_2^+ ion irradiation at several temperatures.

temperature range where beryllium is supposed to be used as a PFM.

5. Helium radiation effects

In general, the accumulation of helium is much harmful to metals than hydrogen because of its strong interaction with lattice defects. Effects of helium ion bombardment have been studied extensively, emphasizing blistering [23]. Helium enhances the formation of bubbles drastically due to the strong bonding to vacancies and their clusters. As a result, local swelling and degradation of mechanical properties of bulk materials take places as well. It was reported that a 200 nm thick surface damaged layer by helium ion irradiation can result in embrittlement at low temperatures and ductility loss at high temperatures for a bulk sample of molybdenum [24].

Fig. 12 demonstrates the difference of damage properties in tungsten irradiated with hydrogen ions and helium ions. The specimens irradiated with 8 keV-D_2^+ and 8 keV-He^+ at room temperature to the fluences of 6.5×10^{19} ions/m^2 and 1.7×10^{19} ions/m^2, respectively, were isochronally annealed under the observation up to 973 K. Though the dpa is comparable (about 0.01 dpa at the peak) interstitial type dislocation loops density of the helium irradiation is more than one order of magnitude higher that that of the hydrogen irradiation. Most of the loops in the hydrogen-irradiated specimen disappear by slipping out from the surface up to 573 K, while those in the helium-irradiated one do not change even at 1300 K. It seems that injected helium atoms enhance the nucleation of interstitial loops and stabilizes them very much.

Fig. 13 shows irradiation temperature dependence of microstructure in molybdenum by 8 keV-He^+ irradiation. Interstitial type dislocation loops are formed at first and then bubbles are formed above 1×10^{21} ions/m^2 at all temperatures examined. The local swelling at 1073 K exceeds 50%. Helium injected sub-surface layer exhibits a sponge-like structure.

To investigate the effect of these extremely dense defects on mechanical properties, nano-indentation tests were carried out. Shown in Fig. 14 are the relative

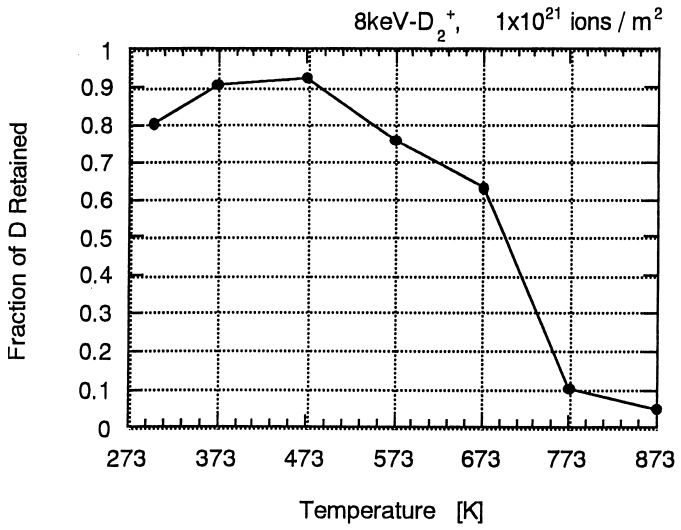

Fig. 11. Fraction of retained deuterium in beryllium irradiated by 8 keV D_2^+ ions to 1×10^{21} ions/m^2 at several temperatures up to 873 K.

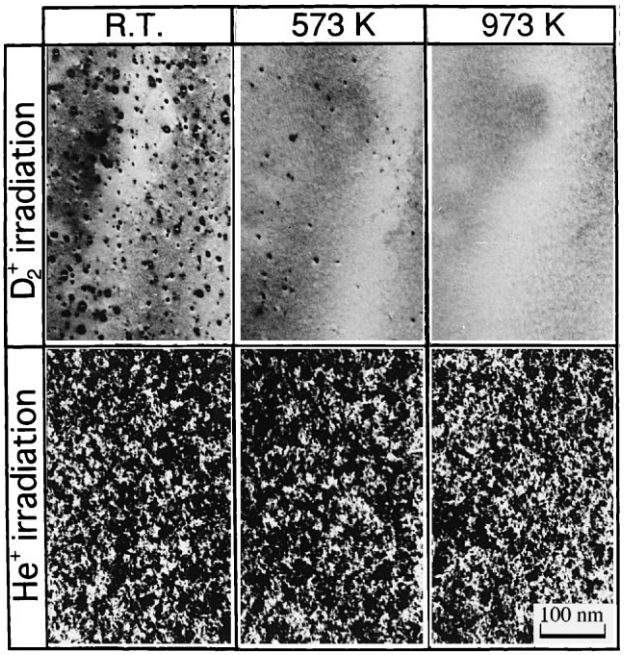

Fig. 12. Comparison of radiation damage in tungsten irradiated by deuterium ions (upper row, 8 keV-D_2^+, 6.5×10^{19} ions/m^2) and helium ions (lower row, 8 keV-He^+, 1.7×10^{19} ions/m^2).

hardness data (H_{irr}/H_{unirr}) of the helium-injected layer [25]. The relative hardness becomes about 1.8 by the formation of dislocation loops and then increases again when the dense fine bubbles are formed at room temperature. At 873 K, on the other hand, the relative hardness becomes about 2.0 by the formation of tangled dislocations but does not increase much by the large bubbles formation. Helium ion irradiation changes the sub-surface layer as well as properties of bulk; TEM disks of 0.1 mm thick become very brittle by the heavy helium irradiation and can be broken often during handling. As such, irradiation embrittlement occurs for the specimens irradiated not only at room temperature but also at 873 K.

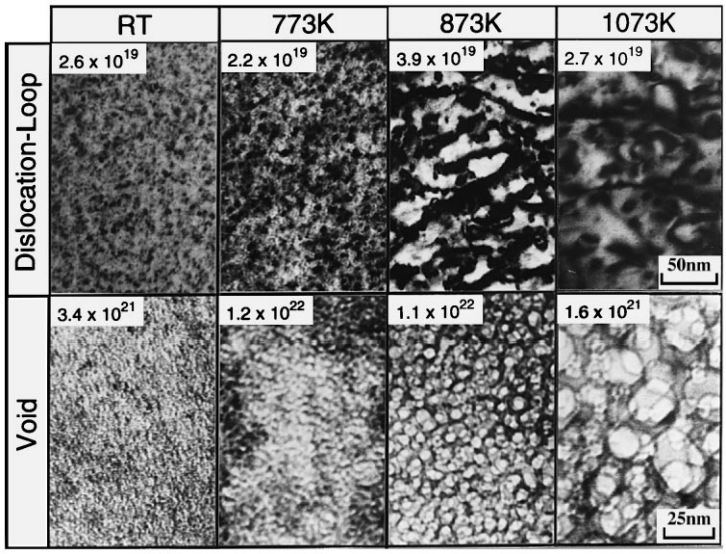

Fig. 13. Microstructural evolution in molybdenum by 8 keV-He^+ ion irradiation at several temperatures up to 1073 K.

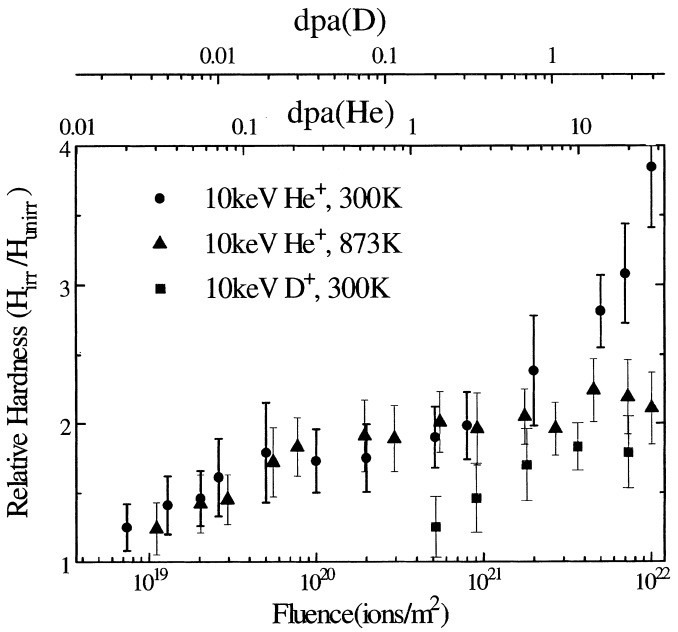

Fig. 14. Hardening of molybdenum by helium and hydrogen ion irradiations [25].

Preliminary measurements on heat-loading, helium ion irradiation enhances the erosion as a synergistic effects of high gas pressure in bubbles, degraded the thermal conductivity of the helium injected layer, ductility loss etc. These results indicate that interaction with helium plasma is a critical issue for high Z metals such as molybdenum and tungsten as PFCs in fusion reactors.

6. Conclusion

Impacts of energetic charge-exchange particles on plasma-wall interaction have been reviewed and discussed, focusing on surface erosion and bulk damage. The walls of plasma facing components of fusion reactors are bombarded with neutral atoms of hydrogen fuel and helium ash created by charge-exchange processes in the edge plasma and also in the core plasma. In the case of charge-exchange neutrals, their interaction with plasma facing components cannot be controlled by magnetic field and their energy spectrum is very wide extending above 10 keV. Therefore bombardment of the neutrals cause an considerable sputtering erosion for the first wall materials directly facing the core plasma, even in tungsten with high sputtering threshold.

Prominent radiation damage by the charge-exchange hydrogen neutrals has been observed in hours-long discharges in TRIAM-1M tokamak. In many metallic materials dislocation loops were accumulated in the subsurface region by the bombardment of keV-range charge-exchange hydrogen neutrals. The flux of the particles was the order of 10^{18} H/m^2/s, which is comparable with that of the energetic neutrals bombarding the first wall of ITER. Severe embrittlement was observed in the long-term tungsten specimen placed in TRIAM-1M. According to ion beam irradiation, damage by energetic hydrogen particles in tungsten seems rather weak at elevated temperatures, while that in beryllium is very severe up to 673 K. The formation of the damage play important role for the retention of hydrogen isotopes. It is anticipated that energetic hydrogen neutrals in fusion devices cause not only sputtering but also material degradation at the sub-surface region and in bulk.

Due to their strong interaction with lattice defects, helium atoms cause much stronger effects on material properties than hydrogen atoms in metals. Defect accumulation by the keV-range helium ions induces significant hardening and embrittlement even at high temperatures. We should pay more attention to the material degradation by energetic helium bombardment, which may affect the stability and reliability of PFMs.

References

[1] ITER, ITER EDA Documentation Series, No. 7, IAEA, Vienna (1996).
[2] D. Post, private communication.
[3] T. Ando, H. Takatsu, H. Nakamura, M. Yamamoto, K. Kodama, T. Arai, M. Shimizu, K. Fukaya, M. Eto, T. Oku, J. Nucl. Mater. 179–181 (1991) 339.

[4] V. Philipps, E. Vietzke, H. Trinkaus, J. Nucl. Mater. 179–181 (1991) 25.
[5] M. Mayer, R. Behrisch, P. Andrew, A.T. Peacock, J. Nucl. Mater. 241–243 (1997) 469.
[6] S. Veprek, M.D. Wiggins, R. Gotthardt, J. Nucl. Mater. 140 (1986) 28.
[7] K. Tokunaga, T. Muroga, Y. Miyamoto, T. Fujiwara, N. Yoshida, K. Nakamura, N. Hiraki, S. Itoh and the TRIAM Group, J. Nucl. Mater. 179–181 (1991) 356.
[8] N. Yoshida, A. Nagao, K. Tokunaga, K. Tawara, T. Muroga, T. Fujiwara, S. Itoh and the TRIAM Group, Radiation Effects and Defects in Solids 124 (1992) 99.
[9] K. Tokunaga, T. Muroga, T. Fujiwara, K. Tawara, N. Yoshida, S. Itoh and the TRIAM Group, J. Nucl. Mater. 191–194 (1992) 449.
[10] Y. Hirooka, M. Bourham, J.N. Brooks, R.A. Causey, G. Chevalier, R.W. Conn, W.H. Eddy, J. Gilligan, M. Khandagle, Y. Ra, J. Nucl. Mater. 196–198 (1992) 149.
[11] Y. Hirooka, these Proceedings.
[12] A. Thoma, K. Asmussen, R. Dux, K. Krieger, A. Herrmann, B. Napiontek, R. Neu, J. Steinbrink, M. Weinlich, U. Wenzel and the ASDEX Upgrade Team, Plasma Phys. Control. Fusion 39 (1997) 1487.
[13] Y. Hirooka, J. Won, R. Boivin, D. Sze, V. Neumoin, J. Nucl. Mater. 230 (1996) 173.
[14] Y. Hirooka, Fusion Eng. Design 37 (1997) 299.
[15] H.Y. Guo, J.P. Coad, S.J. Davies, J.D. Elder, L.D. Horton, X.L. Li, J. Lingertat, A. Loarte, G.F. Matthews, R.D. Monk, R. Simonini, M.F. Stamp, P.C. Stangeby, A. Tabasso, J. Nucl. Mater. 241–243 (1997) 385.
[16] S. Itoh, N. Hiraki, Y. Nakamura, K. Nakamura, A. Nagao, S. Moriyama, T. Fujita, E. Jotaki, S. Kawasaki, in: Plasma Physics and Controlled Nuclear Fusion Research, vol. 1, IAEA, Vienna, 1991, p. 733.
[17] S. Itoh, K. Nakamura, M. Sakamoto, K. Makino, E. Jotaki, S. Kawasaki, H. Nakashima, T. Yamagajo, Proceedings of the 16th IAEA Fusion Energy Conference (Montreal), 1996, IAEA-CN-64/EP-6.
[18] T. Hirai, K. Tokunaga, T. Fujiwara, N. Yoshida, S. Itoh and the TRIAM Group, these Proceedings.
[19] R. Sakamoto, T. Muroga, N. Yoshida, J. Nucl. Mater. 212–215 (1994) 1426.
[20] R. Sakamoto, T. Muroga, N. Yoshida, J. Nucl. Mater. 220–222 (1995) 819.
[21] P. Lucasson, Fundamental aspects of radiation damage in: M.T. Robinson, F.W. Young Jr. (Eds.), Metals, vol. 1 CONF751006-P1, USERDA, 1975, p. 42.
[22] N. Yoshida, S. Mizusawa, R. Sakamoto, T. Muroga, Fusion Technology, to be published.
[23] M. Kaminsky, Radiation Effects on Solid Surfaces, American Chemical Society, Washington, DC, 1976.
[24] K. Shinohara, A. Kawakami, S. Kitajima, Y. Nakamura, M. Kutsuwada, J. Nucl. Mater. 179–181 (1991) 246.
[25] T. Iwakiri, H. Watanabe, N. Yoshida, these Proceedings.